Bioorganic & Medicinal Chemistry 20 (2012) 6989–7001

Contents lists available at SciVerse ScienceDirect

Bioorganic & Medicinal Chemistry

journal homepage: www.elsevier.com/locate/bmc

Synthesis and docking studies of novel antitumor benzimidazoles

Mohamed A. Omar [a], Yasser M. Shaker [a,*], Shadia A. Galal [a], Mamdouh M. Ali [b], Sean M. Kerwin [c], Jing Li [c], Harukuni Tokuda [d], Raghda A. Ramadan [e], Hoda I. El Diwani [a]

[a] Chemistry of Natural and Microbial Products Department, National Research Center, Dokki, 12311 Cairo, Egypt
[b] Biochemistry Department, Division of Genetic Engineering and Biotechnology, National Research Centre, Cairo, Egypt
[c] Phar-Med Chem, The University of Texas at Austin, 1 University Station, A1935, Austin, TX 78712-0128, USA
[d] Department of Complementary and Alternative Medicine, R&D, Graduate School of Medical Science, Kanazawa University, 13-1 Takara-machi, Kanazawa 920-8640, Japan
[e] Youssef Jameel Science and Technology Research Center, The American University in Cairo, New Cairo, Egypt

ARTICLE INFO

Article history:
Received 24 September 2012
Accepted 11 October 2012
Available online 16 October 2012

Keywords:
Benzimidazoles
Cytotoxicity
Epstein–Barr virus early antigen (EBV-EA) activation
Docking study
Plasminogen activator (uPA) receptor
uPA enzyme

ABSTRACT

In this work, the benzimidazole-pyrrole conjugates **6a–h** and benzimidazole-tetracycles conjugates **12–14** were prepared. The cytotoxicity of the compounds **3**, **4a–h**, **6a–h**, **8**, **10** and **12–14** was tested against lung cancer cell line A549. Compound **6b** exhibited higher activity than the bis-benzoxazole natural product (UK-1), the standard. The tested **4g**,**h**, **6a–h**, **10** and **12–14** exhibited remarkable cytotoxicity activity against breast cancer cell line MCF-7 with higher activity than tamoxifen. Furthermore, compound **4h** was found to be also more potent than doxurubicin. The antitumor promotion activity of synthesized compounds **4g**,**h**, **6a–h**, **10** and **12–14** has been estimated by studying their possible inhibitory effects on EBV-EA activation induced by 12-*O*-tetradecanoylphorbol-13-acetate (TPA). Among the studied compounds, the inhibitory activities of compounds **8**, **13** and **14** demonstrated strong inhibitory effects on the Epstein–Barr virus early antigen (EBV-EA) activation without showing any cytotoxicity on the Raji cells and their effects being stronger than that of a representative control, oleanolic acid.

Moreover, the molecular docking of the new compounds into plasminogen activator (uPA) receptor has been in correlation with the antitumor activity. All synthesized compounds **3**, **4a–h**, **6a–h**, **8**, **10** and **12–14** were docked into same groove of the binding site of the native co-crystalized (4-iodobenzo[*b*]thiophene-2-carboxamidine) ligand (PDB code:1c5x) for activity explaination. Compounds **4h**, **6b** and **13**, giving the best docking results, were further studied to estimate their effect on the level of uPA using AssayMax human urokinase (uPA) ELISA kit. In case of A549 cell line, compound **6** exhibited similar activity to MMC, and for MCF-7 cell line, compound **4h** exhibited similar activity to doxorubicin, in inhibiting the expression of uPA.

1. Introduction

Benzimidazole derivatives are structural isosteres of naturally occurring compounds such as purine, consequently, they can easily interact with biomolecules of the living systems possessing diverse biological activity as well as anticancer effects against various types of cell lines.[1–7] Different modes of action of benzimidazole compounds have been described in the literature, such as DNA groove binding,[8] topoisomerase I,[9–11,8] or II,[12] checkpoint kinase (Chk2)[13–15], polo-like kinase 1[16] inhibition.

Urokinase plasminogen activator (uPA) is a serine protease that functions in the conversion of the circulating plasminogen to the active, broad-spectrum, serine protease plasmin. uPA is secreted as an inactive single-chain proenzyme by many different cell types and exists in a soluble or cell-associated form by binding to a specific membrane uPA receptor (uPAR).[17,18] The uPA is involved in many physiological functions and, along with members of the matrix metalloproteinases (MMPs) family; it has been implicated in cancer invasion and metastatization.[19–21] Besides the proteolytic function, upon binding to uPAR, uPA is involved in initiating versatile intracellular signal pathways that regulate cell proliferation, adhesion, and migration through its interaction with various integrins and vitronectin.[22] Urokinase is implicated in a large number of malignancies, for example, cancers of breast, lung, bladder, cervix, kidney, stomach and brain.[23,24] The role of uPA in human cancer progression is further supported by clinical evidences demonstrating that high tissue levels of its components correlate with a poor prognosis in different types of cancer as breast, gastrointestinal carcers.[25,26]

In the literature, benzimidazole-heterocycles conjugates linked at the 2-position were synthesized and evaluated for their antitumor activity. Coupling of benzimidazole-4-carboxamide to 1-propylpiperidin-4-yl at the 2-position of the benzimidazole, i.e. compound **I** (Fig. 1), has been discovered to display a very good

* Corresponding author. Tel.: +20 233371615; fax: +20 23337093.
E-mail address: yabdelrahman@yahoo.com (Y.M. Shaker).

0968-0896/$ - see front matter © 2012 Elsevier Ltd. All rights reserved.
http://dx.doi.org/10.1016/j.bmc.2012.10.010

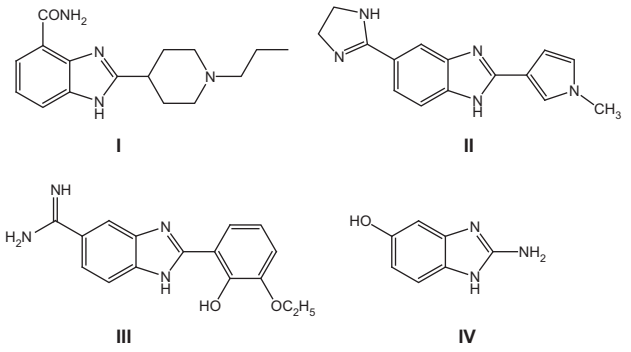

Figure 1.

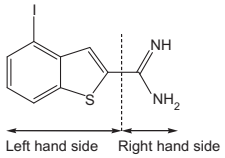

Figure 2.

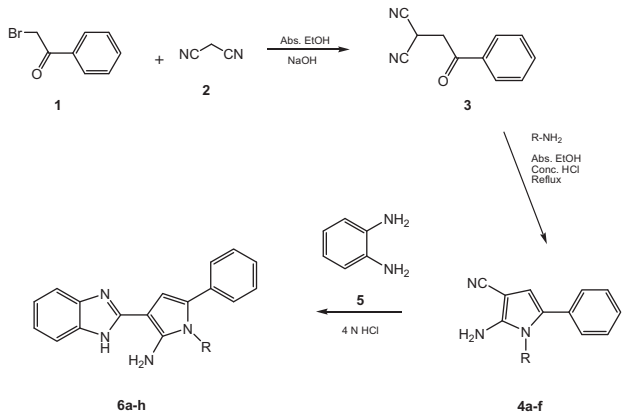

	R
a	2-pyridyl
b	4-pyridyl
c	3-bromophenyl
d	4-bromophenyl
e	3-chlorophenyl
f	4-chlorophenyl
g	2-benzimidazolyl
h	2-methylbenzimidazolyl

Scheme 1.

potency against poly(ADP-ribose)polymerase (PARP), possessing oral efficacy in several preclinical murine tumor models potentiating the efficacy of radiation and many cytotoxic agents e.g. temozolomide and *cis*-platin.[27]

Heterocyclic benzimidazole derivatives bearing amidino substituents at C-5 of benzimidazole ring have been prepared by introducing pyridine, imidazole or N-methylpyrrole at C-2 as in compound **II** (Fig. 1), which was found to be the most potent antitumor one.[28]

Benzimidazole derivatives were found to be active as urokinase plasminogen activator inhibitors as 2-(2-hydroxy-3-ethoxyphenyl)-1*H*-benzimidazole-5-carboxamidine **III**,[29] 2-aminobenzimidazole and 2-amino-5-hydroxybenzimidazole **IV** (Fig. 1).[30]

Based on bioisosterism theory, we had for target in this manuscript the synthesis of benzimidazoles acting as urokinase inhibitors as analogues to the lead compound, 4-iodobenzo[*b*]thiophene-2-carboxamidine (B428, IC_{50} value of 320 nM,Fig. 2).[31–35] B428 is a potent and selective inhibitor of the plasminogen activator urokinase.[36] In our syntheses, the left-hand side of the lead compound was changed to benzimidazole and the right-hand side to substituted 2-aminopyrroles or the highly basic and hydrophobic quinoxalino-1,4-benzodiazepine moiety. We aimed to increase the number of amidine skeleton in the stucture of the new compounds due to its important role in activity.[36]

The cytotoxicity of the new compounds against breast cancer, MCF-7, human lung adenocarcinoma, A549 and the in vitro promoting activity by estimating the inhibitory effect on Epstein–Barr virus early antigen (EBV-EA) activation was tested as well as the effect of structure variation on activity was studied. Successfuly, the activity of all the compounds against MCF-7, except compound **6c**, was higher than tamoxifen, especially compound **4h**, which was found to be more potent than tamoxifen and doxurubicin, and was chosen for further optimization. Also compounds **8**, **13** and **14** were potent against Burkitt's lymphoma Epstein-Barr virus, and most of the compounds express high activity against human adenocarcinoma. The new class of 2-substituted benzimidazoles by the quinoxalino-1,4-diazepine moiety was discovered to be of interesting antitumor activity. Molecular docking studies have been performed to explain activity and to find out the possible interaction between the synthesized compounds and Urokinase plasminogen activator (uPA) receptor (uPAR). The high molecular docking scores of the new compounds into uPAR was in correlation with the potent antitumor activity of the new compounds. Compounds **4h**, **6b** and **13**, giving the best docking results, were further studied to estimate their effect on the level of uPA using AssayMax human urokinase (uPA) ELISA kit. In case of A549 cell line, compound **6** exhibited similar activity to MMC, and for MCF-7 compound **4h** exhibited similar activity to doxorubicin, in inhibiting the expression of uPA.

2. Results and discussion

2.1. Chemistry

Compound **3** was prepared by the dehydrohalogenation reaction of phenacyl bromide **1** and malononitrile **2** as previously reported.[37] Cycloaddition of various aromatic and heteroaromatic amines to compound **3** was accomplished in the presence of few drops of conc. hydrochloric acid in ethanol, to afford the 2-amino-3-cyano-5-phenyl pyrrole derivatives **4a**–**h**.[38] Compounds **4a**–**h** were used as starting materials to prepare the desired 2-pyrrolylbenzimidazole derivatives. Refluxing **4a**–**h** with *o*-phenylenediamine **5** in 4 N HCl, followed by neutralization with NH_4OH, yielded 3-(1*H*-benzimidazol-2-yl)-5-phenyl-1-(aryl)- 1*H*- pyrrol-2-amine **6a**–**h** (Scheme 1).

The formation of the novel bis-benzimidazoles **6g** and **6h** was performed by using the same strategy. The reaction of **3** with 2-aminobenzimidazole or 2-aminomethylbenzimidazole yielded compounds **4g** and **4h** which were further reacted with *o*-phenylenediamine **5** in presence of 4 N HCl to form **6g** and **6h**, respectively (Scheme 1).

3-Amino-1*H*-quinoxalin-2-one **8**,[39] prepared previously by refluxing *o*-phenylenediamine **5** with ethyl oxamate **7** in pyridine, was cyclocondensed with anthranilic acid **9** to afford the tetracyclic product **10** (Scheme 2).[40] Introduction of 2-benzimidazolylmethyl moiety into the quinoxalinyl NH of compound **10**, was

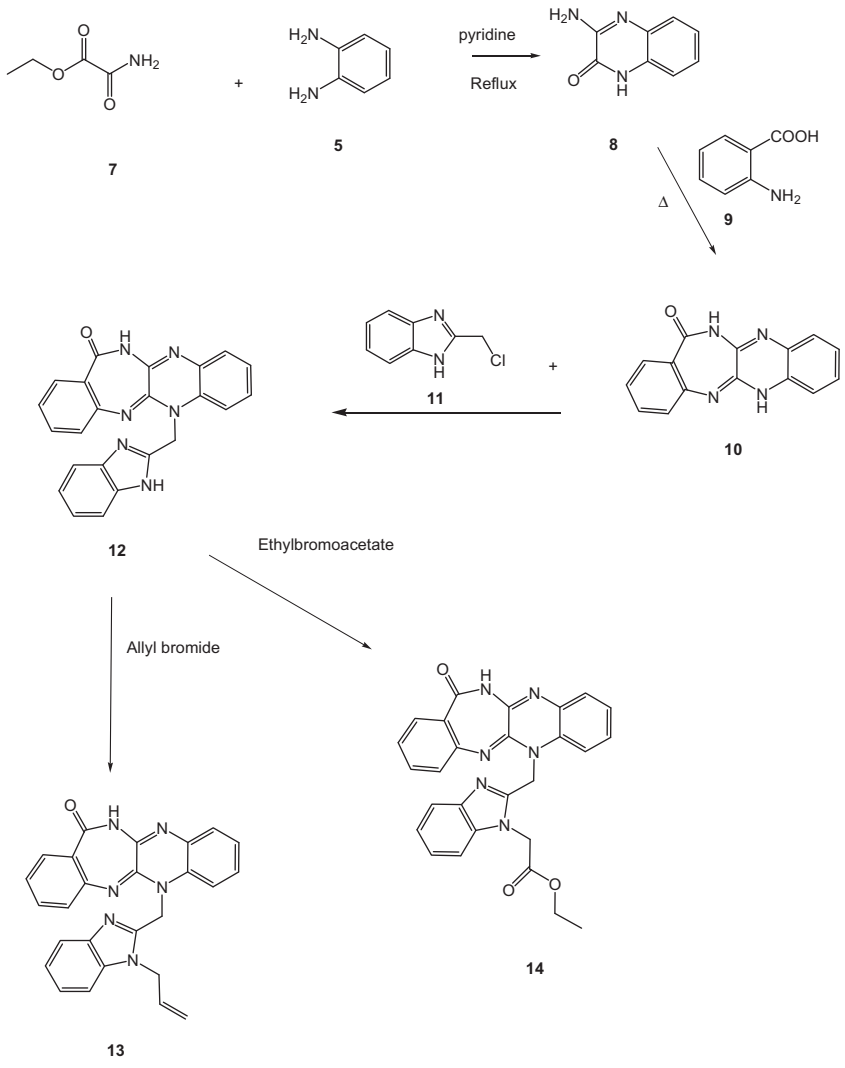

Scheme 2.

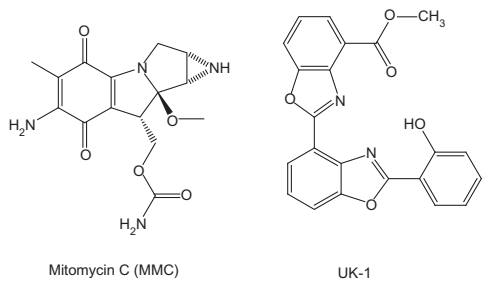

Figure 3.

achieved by its reaction with 2-chloromethylbenzimidazole **11**[41] in DMF and anhydrous potassium carbonate to form the desired product **12**. Subsequent alkylation of **12** with allyl bromide and ethyl bromoacetate in DMF and anhydrous potassium carbonate yielded **13** and **14** respectively (Scheme 2).

2.2. Antitumor activity

2.2.1. Cytotoxicity against lung cancer cell line A549

The cytotoxicity of the compounds **3**, **4a**–**h**, **6a**–**h**, **8**, **10** and **12**–**14** was tested using the AlamarBlue assay[42] in lung cancer cell line A549. For comparison, mitomycin C (MMC, Fig. 3) and the bis-benzoxazole natural product (UK-1, Fig. 3) were also tested (Table 1). The most active compound **6b** exhibited higher activity than UK-1 (IC_{50} = 1.1 μM). Most of the synthetic intermediates and benzimidazoles were of moderately strong cytotoxicity against A549 cell line, with the exception of the pyrrole derivative **4a**, which has moderate activity. The order of activity of the compounds was **6b**, **13**, **4d**, **6h**, **6e**, **4f**, **6g**, **4e** = **6a**, **14**, **12, 8**, **3**, **6f** in a descending order**.**

2.2.2. Cytotoxicity against breast cancer cell line MCF7

Cytotoxicity of compounds **4g**, **4h**, **6a**–**h**, **10** and **12**–**14** was tested using by SRB assay using the method of Skehan et al[43] in breast cancer cell line MCF-7. For comparison doxorubicin (DOX) and tamoxifen (TAM) (Fig. 4) were also tested (Table 2). All of the tested compounds exhibited higher activity than tamoxifen, and compound **4h** was more potent than doxorubicin. The order of reactivity was **4h**, **13**, **6b**, **6d**, **6f** = **14**, **6a**, **6h**, **4g**, **10**, **6g**, **6e**, **12**, **6c** in a descending order (Table 2).

2.2.3. Antitumor promoting effect in vitro (Inhibition of Epstein–Barr virus activation test)

A primary screening test was carried out using a short-term in vitro synergistic assay on Epstein–Barr virus early antigen

Table 1
The cytotoxicity of compounds **3**, **4a–h**, **6a–h**, **8**, **10**, **12–14** as well as Mitomycin C (MMC) and UK-1 against A549 cell line

Compound	IC_{50} for A549[a] (μM)
3	9.7 ± 4.2
4a	32.0 ± 19.2
4b	10.7 ± 2.8
4c	13.0 ± 2.9
4d	4.6 ± 1.3
4e	8.0 ± 1.5
4f	7.7 ± 0.4
4g	12.1 ± 2.8
4h	12.0 ± 5.2
6a	8.0 ± 1.5
6b	1.1 ± 0.7
6c	13.5 ± 1.2
6d	12.0 ± 2.6
6e	7.0 ± 4.6
6f	9.9 ± 3.9
6g	7.7 ± 2.0
6h	5.1 ± 3.5
8	9.1 ± 0.6
10	13.2 ± 4.5
12	8.5 ± 1.6
13	3.4 ± 0.5
14	8.4 ± 2.2
MMC	0.4 ± 0.1
UK-1	2.0 ± 0.5

Data are expressed as mean ± S.E.of three separate experiments.
[a] Determined using the AlamarBlue assay.[43]

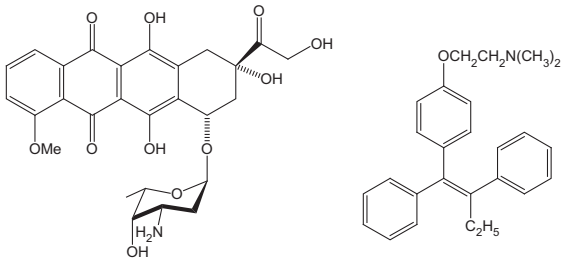

Doxorubicin (DOX) Tamoxifen (TAM)

Figure 4.

Table 2
The cytotoxicity of compounds **4g**,**h**, **6a–h**, **10**, **12–14** as well as doxurubicin and tamoxifen against MCF-7 cell line

Compound	IC_{50} for MCF7 μg/well
4g	1.28
4h	0.515
6a	0.934
6b	0.705
6c	2.12
6d	0.82
6e	1.7
6f	0.934
6g	1.62
6h	0.972
10	1.39
12	1.66
13	0.667
14	0.934
DOX	0.629
TAMOX	1.82

Table 3
The Relative ratio[a] of EBV-EA activation with respect to positive control (100%) in the presence of compounds **4g**,**h**, **6a–h**, **8**, **10**, **12–14** and Oleanolic acid

Compound	Concentration (mol ratio/TPA) % to control (% viability)			
	% to control (% viability) 1000 mol ratio/TPA[bc]	500 mol ratio/ TPA[b]	100 mol ratio/ TPA[b]	10 mol ratio/ TPA[b]
4g	19.7(60)	49.6	83.5	100
4h	18.0(60)	48.3	82.0	100
6a	15.9(60)	47.3	79.1	100
6b	15.3(60)	46.9	78.6	100
6c	19.2(60)	49.9	84.0	100
6d	18.9(60)	48.0	83.2	100
6e	17.8(60)	48.3	80.1	100
6f	20.1(60)	50.3	85.6	100
6g	16.3(60)	48.2	80.0	100
6h	18.7(60)	48.3	82.6	100
8	12.6(70)	46.3	78.1	100
10	22.6(60)	54.6	86.3	100
12	20.5(60)	53.1	85.6	100
13	11.6(60)	45.8	77.9	100
14	10.3(60)	43.7	74.4	100
Oleanolic acid	12.7 (70)	3 0.0	80.0	100

Data are expressed as mean ± S.E. of three separate experiments.
[a] Values represent percentages relative to the positive control value (100%).
[b] TPA concentration was 20 ng/mL (32 pmol/mL).
[c] Values in parentheses are the viability percentages of Raji cells.

(EBV-EA) activation.[44–46] The inhibitory effect of benzimidazole derivatives **4g**,**h**, **6a–h**, **8**, **10** and **12–14** on the EBV-EA activation induced by TPA and the associated viability of Raji cells was listed in Table 3. In this assay, all the tested compounds showed inhibitory effects on EBV-EA activation without cytotoxicity on Raji cells. All compounds exhibited dose dependent inhibitory activities, and the viability percentages of Raji cells treated with the test compounds were 60% or 70% at the highest concentration of 1000 mol ratio/TPA. As shown in Table 3, the inhibitory activities of compounds **8**, **13**, and **14** were stronger at concentration (1,000) than that of oleanolic acid,[47] known as a representive anti-tumor promoting agent. The relative ratio of compound **14** with respect to TPA (100%) was 10.3, 43.7, 74.4 and 100% at the concentrations of 1000, 500, 100 and 10 mol ratio/TPA, respectively, (Table 3); meaning 89.7, 56.3, 25.6% and 0.0% inhibition of the EBV-EA activation by TPA, respectively. Compounds **8** and **13** showed 87.4%, 53.7%, 21.9% and 0% and 88.4%, 54.2%, 22.1% and 0% inhibition of the EBV-EA activation by TPA, respectively, at concentrations of 1000, 500, 100 and 10 mol ratio/TPA.

2.3. Molecular docking study

Investigation of the binding affinity of the new benzimidazole derivatives in to uPA receptor (PDB code:1c5x) was performed for the purpose of lead optimization and to find out the interaction between the new synthesized benzimidazole compounds and Urokinase plasminogen activator receptor.

Molecular modeling calculations and local docking were done using MOE[48] (molecular modeling environment) to evaluate the binding free energies of these inhibitors into the target to uPA receptor.

2.3.1. Validation of the docking performance and accuracy

To validate the docking accuracy of the program used, docking of the native co-crystallized (4 (4-iodobenzo[*b*]thiophene-2-carboxamidine) ligand was done into its binding site of uPA receptor.

The docked ligand was exactly superimposed on the native co-crystallized one with RMSD being 0.32 Å and binding free energies of −13.3818 kcal/mol. The hydrogen bonds between the docked li-

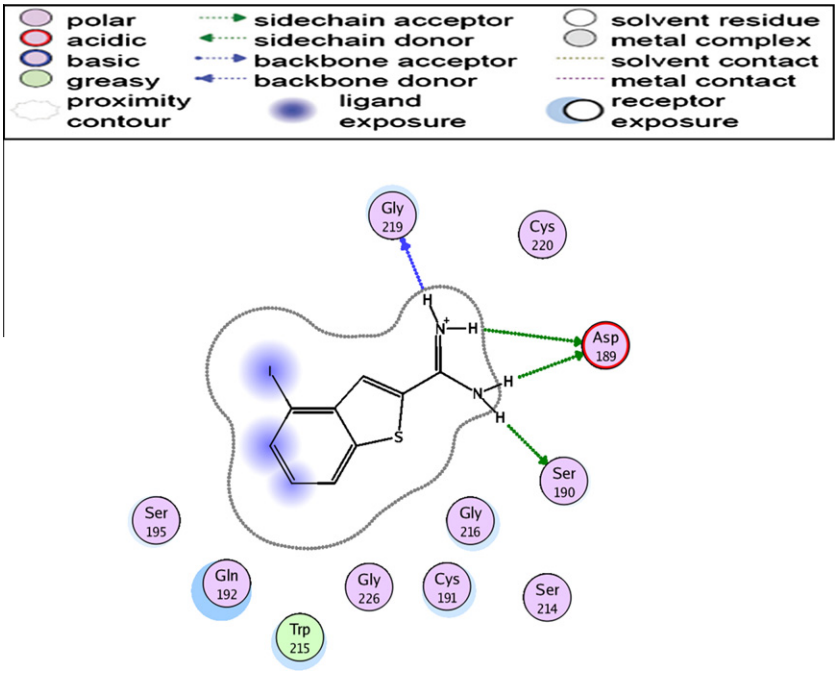

Figure 5. The interaction between the native ligand (4-iodobenzo[*b*]thiophene-2-carboxamidine) with uPA receptor, it exhibit 4 H-bonds with SER 190,GLY 219 and 2 with ASP 189.

gand and the amino acids were the same as those between the native ligand and the amino acids (Fig. 5).

2.3.2. The binding affinities of the synthesized compounds into uPA receptor

Molecular docking study was performed to find out interactions between ligand and receptor and to compare affinities of the synthesized compounds to the target uPA receptor.

For docking calculations, the protein structure (PDB code:1c5x) was first separated from the inhibitor molecule and refined using molecular minimization with added hydrogens.

Docking calculations were carried out using standard default variables for the MOE program.[48] The binding affinity was evaluated by the binding free energies (S-score, kcal/mol) and hydrogen bonds.

All synthesized compounds were docked into same groove of the binding site of the native co-crystalized (4-iodobenzo[*b*]thiophene-2-carboxamidine) ligand.

The affinity of the compounds is represented in Table 4 with the hydrogen bonds with the target receptor.

The compounds giving the best docking scores, based on the binding free energy and the H-bonds with their distance between the amino acids in the receptor, were compounds **4h**, **6a**, **6b**, **6g**, **13** and **14**.

Most of the synthesized compounds gave higher score than the native (4-iodobenzo[*b*]thiophene-2-carboxamidine) which binding free energy was −13.3818 Kcal/mol, while the score of binding free energy of most of the new synthesized compounds was around −15 Kcal/mol. H-bonds between all synthesized compounds and the amino acids in uPA were the same of those between the native co-crystalized ligand with the amino acids of the receptor.

The active-site residues in uPA are Cys42, His57, Asp189, His99, Asp194, Ser190, Ser195, and GLY 219. These residues of uPA are the important residues in S1 site. Most of the synthesized compounds form H-bonds with His 57, Ser 190, Asp 189 and Ser 195 (Figs. 6–8).

The docking results of compounds **4h** and **13** are highly correlated to their antitumor MCF7 activities. Compounds **4h** and **13** are deeply embedded into the binding cleft of uPA receptor domain in S1 pocket with S-score of −16.6664 kcal/mol for compound **4h** and −17.0890 kcal/mol for compound **13**. Also, Compound **4h** and **13** has the lowest binding free energy 16.6664 kcal/mol for compound **4h** and −17.0890 kcal/mol for compound **13** (highest affinity) and has highest biological activity (IC50:0.515 μg/well and IC50:0.667 μg/well) for compounds **4h** and **13**, respectively. For compounds **6b** and **13** their docking results are highly correlated to their antitumor activity against A549 cell lines and compound **6b** is deeply embedded into the binding cleft of uPA receptor domain in S1 pocket with S-score of −16.3476 kcal/mol and IC_{50} of 1.1 ± 0.7 μM. The docking orientations for Compound **13** and compound **6b** along with the native ligand into uPA receptor are represented (Fig. 8).

The overall correlation between the binding free energy (*S*) and the biological activity of the synthesized compounds against MCF-7 is shown in Figure 9. Most of the synthesized compounds' biological activities are correlating with their binding free energy.

Hydrophobic interaction between the ligand and the receptor also indicate good fitting of the compound in the binding site, our compound show good corresponding between their hydrophobic moieties and the hydrophobic alpha spheres found in the binding site of uPA.

2.4. The level of uPA protein expression

The compounds giving the best docking results, **4h**, **6b** and **13** by binding to uPA receptor were further used to estimate their effects on the level of uPA using AssayMax human urokinase (uPA) ELISA kit (Assaypro, USA).

The level of uPA protein expressed in cell extracts of A549 and MCF7 cell lines was represented in Tables 5 and 6.

The level of uPA protein expressed in cell extracts of A549 and MCF7 cell lines was represented in Tables 5 and 6.

In case of A549 cell lines, the concentration of uPA protein reduced in a dose-dependent manner when the cells treated with gradual doses of compounds **6b** and **13** ranged from 0 to the

Table 4
Docking scores of the synthesized benzimidazole compounds into uPA receptor

Compound	S-score (kcal/mol)	K_i value	Hydrogen bonds between atoms of compounds and amino acids				
			Atom of compound	Involved receptor atoms	Involved receptor residues	Type of Hydrogen bond	Distance (Å)
(Native ligand)	−13.3818	1.51 E-10	H 4086	OD 3165	ASP	H-don	2.11
			H 4088	OD 3164	189 ASP	H-don	1.99
			H 4087	OG 3175	189	H-don	2.11
			H 4085	O 3564	SER 190 GLY 219	H-don	1.81
3	−12.9846	2.96 E-10	O 5131	NE 840	HIS 57	H-acc	2.73
			O 5131	OG 3232	SER 195	H-acc	2.80
4a	−14.2778	3.33 E-11	—	—	—	—	—
4b	−15.1534	7.59 E-12	N 5150	NE 840	HIS 57	H-acc	3.04
4c	−15.5169	4.11 E-12	—	—	—	—	—
4d	−15.6518	3.27 E-12	N 5122	OG 3175	SER 190	H-acc	2.65
4e	−15.8661	2.27 E-12	—	—	—	—	—
4f	−15.6487	3.29 E-12	N 5122	OG 3175	SER 190	H-acc	2.66
4g	−15.6977	3.02 E-12	—-	—	—	–	—
4h	−16.6664	5.89 E-13	N 5128	OG 3232	SER 195 HIS 57	H-don	2.62
			N 5128	NE 840	SER 195	H-acc	2.89
			N 5128	OG 3232		H-acc	2.62
6a	−15.2428	6.53 E-12	H 5116	O 3184	CYS 191	H-don	1.90
			H 5115	OG 3232	SER 195	H-don	2.07
			N 5111	NE 840	HIS 57	H-acc	2.60
6b	−16.3476	1.00 E-12	N 5108	OG 3232	SER 195 SER 195	H-don	2.78
			N 5108	OG 3232		H-acc	2.78
6c	−14.8792	1.2 E-11	N 5110	NE 840	HIS 57	H-acc	2.95
6d	−14.9337	1.1 E-11	H 5121	OG 3232	SER 195	H-don	1.68
6e	−15.4696	4.4 E-12	N 5110	N 3208	GLY 193	H-acc	3.12
6f	−15.5963	4.45 E-12	N 5110	N 3208	GLY 193	H-acc	3.08
6g	−16.1000	1.53 E-12	H 5122	OG 3232	SER 195	H-don	2.63
6h	−15.8928	2.17 E-12	H 5123	OG 3232	SER 195	H-don	2.16
			N 5136	NE 840	HIS 57	H-acc	2.55
8	−10.4686	2.08 E-8	H 5114	OD 3164 OG 3175	ASP 189	H-don	1.95
			H 5113	O 3564	SER 190	H-don	1.45
			H 5109		GLY 219	H-don	1.91
10	−12.0956	1.33 E-9	H 5118	OG 3232	SER 195	H-don	1.98
			O 5119	NE 840	HIS 57	H-acc	2.73
			O 5119	OG 3232	SER 195	H-acc	2.65
12	−15.2572	6.36 E-12	N 5131	OG 3232	SER 195	H-don	2.24
			N 5131	OG 3232	SER 195	H-acc	2.24
13	−17.0890	2.88 E-13	N 5116	NE 840	HIS 57	H-acc	2.67
14	−16.0152	1.7 E-12	N 5131	OG 3232	SER 195	H-acc	2.50

S- score: binding free energy.
Native Ligand: The native co-crystallized (4-iodobenzo[*b*]thiophene-2-carboxamidine) bound ligand of uPA (PDB code:1c5x).
K_i value = Exp (delta G/RT).
R = 1.986 cal/mol-K, T = 298 K.

IC_{50}. For compound **6b**, the uPA concentration of untreated cells (control) was 11.00 ± 1.60 ng/ml, while that of cells treated were 6.20 ± 0.75, 5.20 ± 0.65, 4.80 ± 0.50 and 2.70 ± 0.30 ng/ml, respectively (Table 5), this mean that the level of uPA decreased by 44%, 53%, 56% and 75%, respectively, when compared with control. For compound **13**, the uPA concentration of untreated cells (control) was 11.00 ± 1.60 ng/ml, while that of cells treated were 7.40 ± 0.85, 6.20 ± 0.72, 5.30 ± 0.50 and 3.80 ± 0.45 ng/ml, respectively, (Table 5) and they decreased by 33%, 44%, 52% and 65% as compared with control. From the result, compound **6b** exhibited higher activity than compound **13** and similar to mitomycin in inhibition the expression of uPA.

In case of MCF7 cell line, the concentration of uPA protein reduced in a dose-dependent manner when the cells treated with gradual doses of compounds **4h** and **13** ranged from 0 to the IC_{50}. For compound **4h**, the uPA concentration of untreated cells (control) was 11.40 ± 1.40 ng/ml, while that of cells treated were 7.40 ± 0.80, 5.70 ± 0.63, 4.00 ± 0.45 and 2.80 ± 0.30 ng/ml, respectively, with 35%, 50%, 65% and 75% decrease level as compared with control. For compound **13**, the uPA concentration of untreated cells (control) was 11.40 ± 1.40 ng/ml, while that of cells treated were 8.80 ± 1.20, 7.70 ± 0.85, 7.00 ± 0.80 and 4.40 ± 0.50 ng/ml, respectively (Table 6) and they showed 23%, 33%, 39% and 61% decrease level, respectively, comparing to control. From the foregoing results, compound **4h** exhibited higher activity toward suppression the expression of uPA than compound **13** and it was similar to doxorubicin in inhibition the expression of uPA.

3. Structure-activity relationship

Regarding adenocarcinoma inhibition, the most active compound was found to be **6b**, having the 4-pyridyl as substituent in position 1 of the pyrrole ring which may act as hydrogen bonding acceptor. The role of the N atom of the pyridine ring was also proven by the decrease in activity if the position of N atom in pyridine differs with respect to the link to pyrrole as **6a** having the 2-pyridyl ring was less potent than **6b** having the 4-pyridyl ring. The pronounced cytotoxicity of benzimidazole derivative **6b** relative to the pyrrolo intermediate **4b** was remarkable, indicating the importance of the contribution of the benzimidazole moiety in activity. Compound **13** having the quinoxalinobenzodiazepine moiety as well as the allyl group on the N atom of the benzimidazole moiety, was the 2nd most potent compound in the series. The importance of benzimidazole substitution to the tetracyclic scaffold as well as

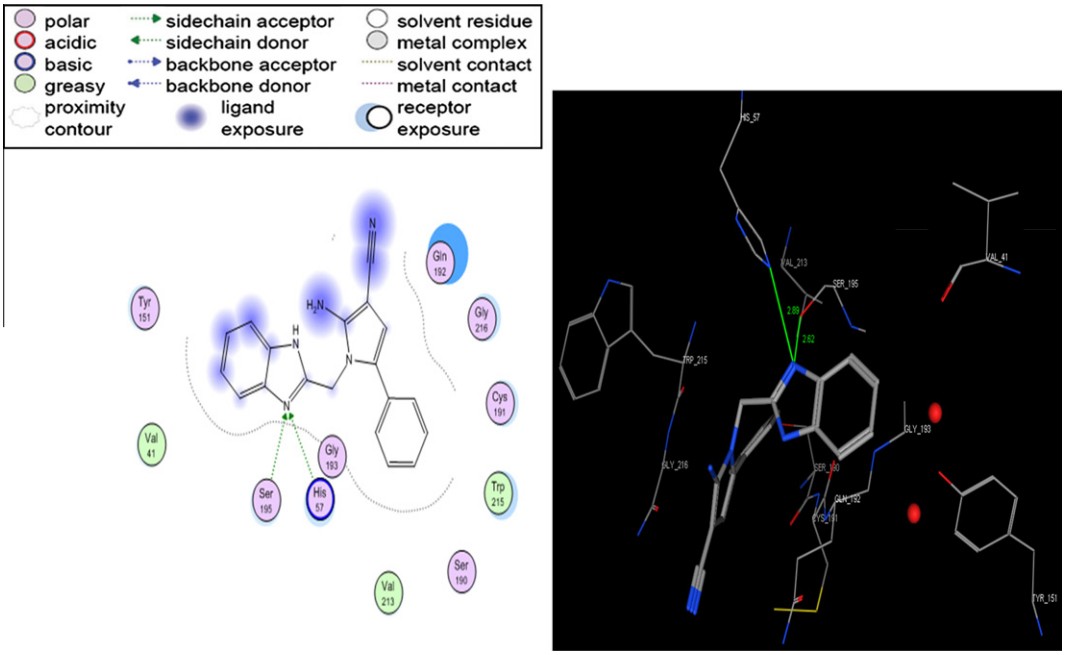

Figure 6. Ligand interaction and the binding mode of compound **4h** with uPA receptor, it exhibited 2 H-bonds with SER 195 and 1 H-bond with HIS 57. The hydrogen bond formed is colored in green.

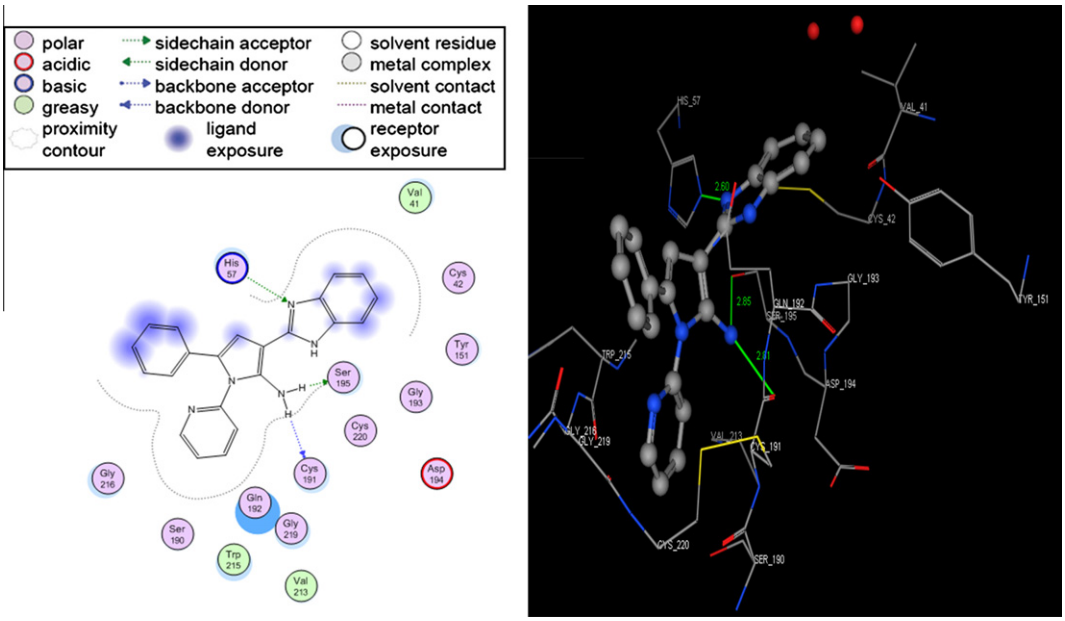

Figure 7. Ligand interaction and the binding mode of compound **6a** with uPA receptor, it exhibited 3 H-bond with CYS 191, SER 195 and HIS 57. The hydrogen bond formed colored in green.

the allyl substitution on the benzimidazole NH were emphasized by the fact that **12** was more potent than **10** and **13** was more potent than **12**, respectively. The reason of this activity may be discovered from the docking of compounds **6b** and **13** which showed that they were found to be deeply embedded into the binding cleft of the uPA receptor domain. Also the allyl substitution on the benzimidazole NH was more favored than the ethyl acetate substitution as **13** was more potent than **14**.

Substitution of the pyrrole ring of compound **6e** by 3-chlorophenyl was more favoured than substitution by 4-chorophenyl as for compound **6f**, as **6e** was more potent than **6f**. Also, the chlorophenyl substitution was more favoured than the bromophenyl as **6f** and **6e** were more potent than **6d** and **6c**, which may be attributed to the larger volume of Br with respect to Cl.

Compound **4h** was found to be highly potent against MCF-7. This may be due to the presence of the hydrophobic phenyl group, the polar and hydrogen bond donor NH_2 group and the electron withdrawing CN group. Also the CH_2 linker between the benzimidazole moiety and the pyrrole ring might also have a certain influence on activity, as **4h** and **6h** were more potent than **4g** and **6g** respectively. This may be attributed to the hydrophobic interaction of the benzimidazole moiety with the active site of the enzyme, due to more flexibility when linked to CH_2 group. Replacement of the pyrrole ring with the quinixalinobenzodiazepine moiety was

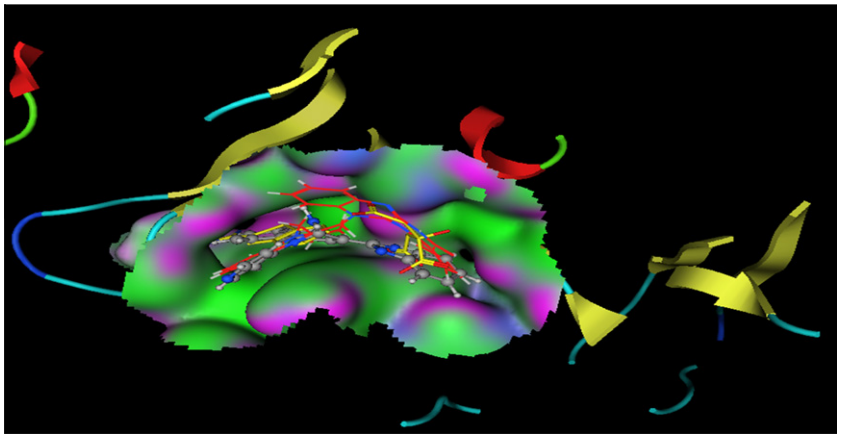

Figure 8. Docking orientations for Compound **13** colored in red and compound **6b** in ball and stick mode along with the native ligand colored in yellow into uPA receptor. A Gaussian Contact surface is drown around the binding site, this is the surface that surrounds the van der Waals surface of a molecule (filling in solvent inaccessible gaps).

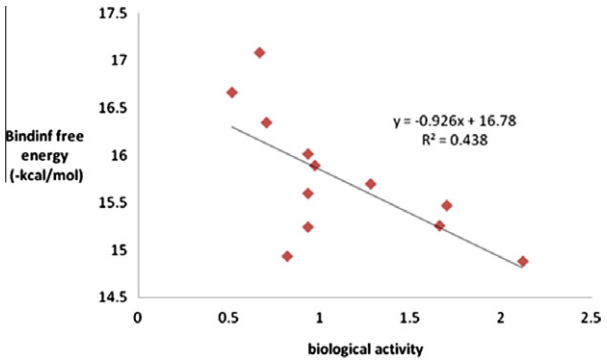

Figure 9. The overall correlation between the binding free energy S and the biological activity synthesized compounds against MCF7.

Table 5
The level of uPA protein measured by ELISA after exposure the A549 cells to gradual concentration of compounds **4h**, **6b**, **13** and mitomycin C (MMC).

Compound	Concentration μM	uPA level (ng/ml)
4h		
	0	11.00 ± 1.60
	1,5	11.6000 ± 1.30
	3	9.7000 ± 1.20
	6	9.8000 ± 1.50
	12	9.2000 ± 1.15
6b		
	0	11.0000 ± 1.60
	0.137	6.2000 ± 0.75[a]
	0.275	5.2000 ± 0.65[a]
	0.55	4.8000 ± 0.50[a]
	1.10	2.7000 ± 0.30[a]
13		
	0	11.0000 ± 1.60
	0.425	7.4000 ± 0.85[a]
	0.85	6.2000 ± 0.72[a]
	1.70	5.3000 ± 0.50[a]
	3.40	3.8000 ± 0.45[a]
MMC		
	0	11.0000 ± 1.60
	0.05	4.3000 ± 0.50[a]
	0.10	3.3000 ± 0.40[a]
	0.20	2.6000 ± 0.20[a]
	0.40	2.4000 ± 0.30[a]

Data are expressed as mean ± S.E. of three separate experiments.
[a] Is significant difference from control untreated at p <0.05.

Table 6
The level of uPA protein measured by ELISA after exposure the MCF7 cells to gradual concentration of compounds **4h**, **6b**, **13** and doxorubicin (DOX)

Compound	Concentration μg/well	uPA level (ng/ml)
4h		
	0	11.4000 ± 1.40
	0.0625	7.4000 ± 0.80[a]
	0.125	5.7000 ± 0.63[a]
	0.25	4.0000 ± 0.45[a]
	0.50	2.8000 ± 0.30[a]
6b		
	0	11.4000 ± 1.40
	0.087	9.8000 ± 1.10
	0.175	8.7000 ± 0.90
	0.35	9.0000 ± 0.86
	0.70	9.4000 ± 0.80
13		
	0	11.4000 ± 1.40
	0.084	8.8000 ± 1.20[a]
	0.167	7.7000 ± 0.85[a]
	0.335	7.0000 ± 0.80[a]
	0.67	4.4000 ± 0.50[a]
DOX		
	0	11.4000 ± 1.40
	0.075	3.4000 ± 0.48[a]
	0.15	3.2000 ± 0.30[a]
	0.30	3.0000 ± 0.35[a]
	0.60	2.7500 ± 0.30[a]

Data are expressed as mean ± S.E. of three separate experiments.
[a] Is significant difference from control untreated at p <0.05.

successful, especially when the benzimidazole has an allyl group or an ethyl acetate group in position1 for compounds **13** and **14**, and the products were more active than tamoxifen. This may also indicate the importance of substitution on the N atom by these two groups which enhance the activity as **13** and **14** were more potent than the unsubstituted compound **12**. The allyl group presence was favored than ethyl acetate group as **13** was more potent than **14**. Similar to the case of adenocarcinoma cytotoxicity, substitution with 4-pyridyl led to higher activity than with 3-pyridyl as **6b** was more active than **6a**. The position of substitution of the halogen atoms on the phenyl ring as the 4-substitution increases the activity more the 3-substitution, as **6d** and **6f** were twice as potent as **6**c and **6e**, respectively.

For the inhibitory effect against Burkitt's lymphoma induced by Epstein virus, the most active compounds were **13** and **14** having the highly hydrophobic quinoxalinobenzodiazepine scaffold linked to the benzimidazole moiety carrying an ester group in the first and an allyl group in the second compound.

Halogen atoms substitution on the phenyl ring of the pyrrole ring of compounds **6c–f** has negative effect on activity within all the tests performed. The role of allyl and ethyl acetate substitution seemed to be crucial for activity as **13** and **14** were twice as potent as their precursor **12**. Also allyl substitution had more positive effect on activity than did the ethyl acetate substitution as **14** was more potent than **13**. The quinoxalino derivative **8**, having NH_2, C=O, NH and C=N, was of high activity. The pyridyl substituted compounds **6a** and **6b** were of moderate activity.

4. Conclusion

New benzimidazole-pyrrole conjugates **6a–h** have been synthesized by the reaction of the synthesized pyrrole derivatives **4a–h** with *o*-phenylene diamine. 3-amino-1*H*-quinoxalin-2-one (**8**) reacted with anthranilic acid (**9**) to form the fused tetracyclic compound **10**. Reaction of 2-chloromethylbenzimidazole (**11**) with compound **10** yielded benzimidazole-tetracyclic conjugate **12**. N-substituted benzimidazoles **13** and **14** were obtained by reaction of compound **12** with halo compounds. The antitumor activity of new benzimidazole conjugates has been evaluated by studying their cytotoxicity against lung cancer cell line A549 and breast cancer cell line MCF-7 besides their inhibitory effects on Epstein–Barr virus early antigen (EBV-EA) activation. One of the tested compounds against lung cancer A549, **6b**, was found to be more potent than mitomycin C. Most of the tested compounds against breast cancer MCF7 cell line showed higher activity than tamoxifen and **4h** was of higher potency than doxurubicin. The cancer chemopreventive activity of the new derivatives **4g**, **4h**, **6a–h**, **10** and **12–14** has been estimated by studying their inhibitory effects on Epstein–Barr virus early antigen (EBV-EA) activation induced by 12-*O*-tetradecanoylphorbol-13-acetate (TPA). The tested compounds showed dose dependent inhibitory activities, most of them showed significant activity at the highest concentration of 1000 mol ratio/TPA. Compounds **14**, **13**, and **8** showed stronger effect than that of oleanolic acid. The Molecular Docking investigation of the synthesized derivatives was carried out for lead optimization and they were docked into plasminogen activator (uPA) receptor. There was good correlation between the binding free energies (DGb, kcal/mol) predicted by MOE and the antitumor activity of the new compounds against MCF-7. The results of the ELISA study were consistent with the docking results indicating that the anticancer effect of the prepared compounds may exert its anticancer activity by inhibiting uPA. It can be concluded from the results obtained that the tested compounds possess significant anticancer activity comparable to the activity of the commonly used anticancer drugs.

5. Experimental

5.1. Physical measurements

Microanalyses, spectral data of the compounds were performed in the Microanalytical, National Research Centre, Cairo, Egypt. The IR spectra (4000–400 cm^{-1}) were recorded using KBr pellets in a Jasco FT/IR 300E Fourier transform infrared spectrophotometer on a Perkin Elmer FT-IR 1650 (spectrophotometer). The NMR spectra were recorded using Joel EX-270 MHz and 500 MHz NMR spectrophotometers. Chemical shifts are reported in parts per million (ppm) from the tetramethylsilane resonance in the indicated solvent. Coupling constants are reported in Hertz (Hz); spectral splitting partners are designed as follow: singlet (s); doublet (d); triplet (t); multiplet (m). The mass spectra were carried out using Finnigan mat SSQ 7000 (Thermo. Inst. Sys. Inc., USA) spectroscopy at 70 ev.

5.1.1. General procedure for the preparation of compounds (4a–h)

A mixture of hetero/aromatic aniline (20 mmol) and 3–5 drops of conc. hydrochloric acid was added to a solution of compound **3** (20 mmol) in ethanol (50 mL). This mixture was refluxed for 7 h. The reaction mixture was then allowed to cool at room temperature. The precipitate was collected by filtration, dried and recrystallized from appropriate solvent.

5.1.2. 2-Amino-5-phenyl-1-(pyridin-2-yl)-1*H*-pyrrole-3-carbonitrile (4a)

Crystallized from chloroform/methanol (2:5) as a green powder. R_f = 0.27 (petroleum ether/ethyl acetate, 1:1). Yield: (71%); mp 121–132 °C; ^{1}H NMR (DMSO-d_6) δ: 6.29 (s, 1H, CH), 7.13–7.59 (m, 8H, H_4+H_5+H_6+$H_{2'}$–$H_{6'}$), δ 8.2 (br, NH_2, D_2O exchangeable), 8.53 (d, J = 7.45 Hz, 1H, CH pyridine). IR (cm^{-1}): 3439, 3343 (NH_2), 2223 (CN). MS: *m*/*z* 261.0, 2.1% (M^++1); *m*/*z* 232.0, 24.5% (M^+—CN–2H); *m*/*z* 231.0, 100.0% (M^+—CN–3H); *m*/*z* 182.0, 15.4% [M^++1—py]. Anal. Calcd for $C_{16}H_{12}N_4$ (260.11): C, 73.83; H, 4.65; N, 21.52. Found: C, 73.88; H, 4.62; N, 21.49.

5.1.3. 2-Amino-5-phenyl-1-(pyridin-4-yl)-1*H*-pyrrole-3-carbonitrile (4b)

Crystallized from chloroform as a brown powder. R_f = 0.25 (petroleum ether /ethyl acetate, 1:1). Yield: 79%; mp 117–119 °C; ^{1}H NMR (DMSO-d_6) δ: 6.20 (s, 1H, CH), 7.50–7.34 (m, 7H, Aromatic protons), 8.2 (br, NH_2, D_2O exchangeable), 8.62 (d, J = 7.4 Hz, 1H, CH pyridine). ^{13}C NMR (500 MHz, DMSO-d_6): 15.33, 66.74, 107.26, 109.31, 116.63, 122.59, 124.55, 128.77, 130.39, 142.34, 164.55. IR (cm^{-1}): 3414, 3325 (NH_2), 2257 (CN). MS: *m*/*z* 260.0, 1.9% (M^+); *m*/*z* 184.0, 5.3% (M^+—Ph); *m*/*z* 168.0, 10.6% [M^+—Ph—NH_2], *m*/*z* 140, 7.7% [M^+ — Ph — NH_2—CN—2H]. Anal. Calcd for $C_{16}H_{12}N_4$ (260.11): C, 73.83; H, 4.65; N, 21.52. Found: C, 73.79; H, 4.66; N, 21.57.

5.1.4. 2-Amino-1-(3-bromophenyl)-5-phenyl-1*H*-pyrrole-3-carbonitrile (4c)

Crystallized from ethyl acetate as a reddish brown powder. R_f = 0.32 (petroleum ether /ethyl acetate, 1:1). Yield: 75%; m.p. 178–180 °C; ^{1}H NMR (DMSO-d_6) δ: 6.60 (s, 1H, CH), 7.52-7.68 (m, 8H, Aromatic protons), 8.3 (broad band, NH_2, D_2O exchangeable). IR (cm^{-1}): 3370, 3337 (NH_2), 2258 (CN). MS: *m*/*z* 338.0, 100.0% (M^+); *m*/*z* 182.0, 20.5% (M^+—*m*-Br-Ph); *m*/*z* 155.0, 45.4% (M^+—*m*-Br-Ph— CN—1H). Anal. Calcd for $C_{17}H_{12}BrN_3$ (338.02): C, 60.37; H, 3.58; Br, 23.63; N, 12.42 Found: C, 60.39; H, 3.59; Br, 23.71; N, 12.39.

5.1.5. 2-Amino-1-(4-bromophenyl)-5-phenyl-1*H*-pyrrole-3-carbonitrile (4d)

Crystallized from ethyl acetate as a yellow powder. R_f = 0.31 (petroleum ether/ethyl acetate, 1:1). Yield 83%; mp 110–112 °C; ^{1}H NMR (DMSO-d_6) δ 6.45 (s, 1H, CH), δ 6.97 (d, J = 8.1 Hz, 2H, H2+H6Aromatic protons), δ 7.10–7.20 (m, 5H, H3′−H4′+H5′+H3+H5), δ 7.50 (d, J = 8.1 Hz, 2H, H2′+H6′), 8.14 (br, NH_2, D_2O exchangeable). ^{13}C NMR (500 MHz, DMSO-d_6): 14.49, 71.36, 109.13, 116.64, 122.20, 124.34, 127.18, 128.77, 131.18, 132.36, 135.77, 144.99, 149.82. IR (cm^{-1}): 3458, 3379 (NH_2), 2257 (CN). Anal. Calcd for $C_{17}H_{12}BrN_3$ (337.02): C, 60.37; H, 3.58; Br, 23.63; N, 12.42. Found: C, 60.31; H, 3.50; Br, 23.61; N, 12.47.

5.1.6. 2-Amino-1-(3-chlorophenyl)-5-phenyl-1*H*-pyrrole-3-carbonitrile (4e)

Crystallized from ethyl acetate as yellow powder. R_f = 0.29 (petroleum ether/ethyl acetate, 1:1). Yield: 83%; mp 185–187 °C; ^{1}H NMR (DMSO-d_6) δ: 6.41 (s, 1H, CH), 6.94–7.41 (m, 9H, Aromatic protons), 8.42 (br, NH_2, D_2O exchangeable). IR (cm^{-1}): 3440, 3337

(NH_2), 2258 (CN). MS: *m*/*z* 294.0, 100.0% (M^++1); *m*/*z* 257.0, 24.6% (M^+—Cl), *m*/*z* 181.0, 12.6% (M^+—*m*-ClPh). Anal. Calcd for $C_{17}H_{12}ClN_3$ (293.07): C, 69.51; H, 4.12; Cl, 12.07; N, 14.30. Found: C, 59.55; H, 4.14; Cl, 12.02; N, 14.36.

5.1.7. 2-Amino-1-(4-chlorophenyl)-5-phenyl-1*H*-pyrrol-3-carbonitrile (4f)

Crystallized from chloroform as a yellow powder. R_f = 0.34 (petroleum ether/ethyl acetate, 1:1). Yield: 79%; mp 98–100 °C; ^{1}H NMR (DMSO-d_6): δ 6.41 (s, 1H, CH), 7.63–6.78 (m, 9H, Aromatic protons), 8.22 (br, NH_2, D_2O exchangeable). IR (cm^{-1}): 3321, 3225 (NH_2), 2208 (CN). MS: *m*/*z* 294.0, 10.6% (M^++1); *m*/*z* 214.0, 1.8% (M^+—Ph—2H); *m*/*z* 104, 9.5% (M^+—Ph—*p*-ClPh). Anal. Calcd for $C_{17}H_{12}ClN_3$ (293.07): C, 69.51; H, 4.12; Cl, 12.07; N, 14.30. Found: C, 69.55; H, 4.13; Cl, 12.15; N, 14.28.

5.1.8. 2-Amino-1-(1*H*-benzo[*d*]imidazol)-5-phenyl-1*H*-pyrrole-3-carbonitrile (4g)

Crystallized from chloroform as a brown powder. R_f = 0.28 (petroleum ether/ethyl acetate, 1:1). Yield: 82%; mp 122–124 °C; ^{1}H NMR (DMSO-d_6) δ: 6.34 (s, 1H, CH), 7.69–7.33 (m, 9H, Aromatic protons), 8.40 (br, NH_2, D_2O exchangeable) 12.55(br, NH, benzimidazole, D_2O exchangeable). ^{13}C NMR (500 MHz, DMSO-d_6): 18.56, 66.76, 107.25, 114.93, 122.59, 128.75, 134.75, 135.35, 142.34, 164.55, 194.86. IR (cm^{-1}): 3359, 3283, 3206 (NH) and (NH_2), 2258 (CN). MS: *m*/*z* 300.0, 0.89% (M^++1); *m*/*z* 183.0, 29.0% (M^++1—benzimidazole part); *m*/*z* 104, 100.0% (M^++1—benzimidazole part—Ph—2H). Anal. Calcd for $C_{18}H_{13}N_5$ (299.12): C, 72.23; H, 4.38; N, 23.40. Found: C, 72.27; H, 4.40; N, 23.36.

5.1.9. 1-((1*H*-benzo[*d*]imidazol-2-yl)methyl)-2-amino-5-phenyl-1*H*-pyrrole-3-carbonitrile (4h)

Crystallized from chloroform as a green powder. R_f = 0.24 (petroleum ether/ethyl acetate, 1:1). Yield: 4.9 g (73%); mp 131–133 °C; ^{1}H NMR (DMSO-d_6): δ 5.07 (s, 2H, CH_2), 6.21 (s, 1H, CH), 7.56–7.54 (m, 5H, H5+H6+H3′+H4+H5′), 7.68 (d, J = 6.9H_Z,2H, H2′+H6′), 7.68 (d, J = 6.9H_Z, 2H, H4+H7), 8.35 (br, NH_2, D_2O exchangeable), 12.52(br, NH, benzimidazole, D_2O exchangeable). ^{13}C NMR (500 MHz, DMSO-d_6): 18.55, 39.79, 114.96, 128.77, 129.49, 134.78, 135.31,194.89. IR (cm^{-1}): 3411, 3329, 3225 (NH), (NH_2), 2206 (CN), 1677 (C=N). Anal. Calcd for $C_{19}H_{15}N_5$ (313.13): C, 72.83; H, 4.82; N, 22.35. Found: C, 72.79; H, 4.39; N, 2.41.

5.1.10. General procedure for the preparation of compounds (6a–h)

A mixture of *o*-phenylenediamine (0.8 g, 7.5 mmol) and pyrrole derivatives (7.5 mmol) in 4 N HCl (20 mL) was refluxed for 6 h. The reaction mixture was allowed to cool and then neutralized with NH_4OH. The resulting precipitate was filtered off and recrystallized from appropriate solvent.

5.1.11. 3-(1*H*-Benzo[*d*]imidazol-2-yl)-5-phenyl-1-(pyridin-2-yl)-1*H*-pyrrol-2-amine (6a)

Crystallized from ethyl acetate as a yellowish green powder. R_f = 0.18 (petroleum ether/ethyl acetate/methanol, 1:1:1/2). Yield: 1.9 g (70%); mp 170–172 °C; ^{1}H NMR (DMSO-d_6) δ: 6.26 (s, 1H, CH), 7.35–7.45 (m, 12H, Aromatic protons), δ 8.56 (d, J = 4H_Z, 1H, CH pyridine), 8.22 (br, NH_2, D_2O exchangeable), 12.69 (br, NH, benzimidazole, D_2O exchangeable). IR (cm^{-1}): 3455 (NH), 3376, 3325 (NH_2). MS: *m*/*z* 350.0, 1.3% (M^+—1H); *m*/*z* 273.0, 2.4% (M^++1—py); *m*/*z* 259.0, 10.3% (M^++2—Ph–NH_2—1H). Anal. Calcd for $C_{22}H_{17}N_5$ (351.15): Anal. Calcd for $C_{22}H_{17}N_5$ (351.15): C, 75.19; H, 4.88; N, 19.93. Found: C, 75.18; H, 4.79; N, 19.99.

5.1.12. 3-(1*H*-Benzo[*d*]imidazol-2-yl)-5-phenyl-1-(pyridin-4-yl)-1*H*-pyrrol-2-amine (6b)

Crystallized from ethyl acetate as a green powder. R_f = 0.38 (petroleum ether/ethyl acetate/methanol, 1:1:1/2). Yield: 1.9 g (70%); mp 135–137 °C; ^{1}H NMR (DMSO-d_6) δ: 6.09 (s, 1H, CH), 7.80–7.09 (m, 9H, Aromatic protons), 7.98–8.16 (m, 2H, Aromatic protons), 8.22 (br, NH_2, D_2O exchangeable), 8.60 (d, J = 4 Hz 2H, CH pyridine), 12.59 (br, NH, benzimidazole, D_2O exchangeable). IR (cm^{-1}): 3393 (NH), 3323, 3260 (NH_2). Anal. Calcd for $C_{22}H_{17}N_5$ (351.15): C, 75.19; H, 4.88; N, 19.93. Found: C, 75.26; H, 4.85; N, 19.89.

5.1.13. 3-(1*H*-Benzo[*d*]imidazol-2-yl)-1-(3-bromophenyl)-5-phenyl-1*H*-pyrrol-2-amine (6c)

Crystallized from ethyl acetate/methanol (2:5) as a brown powder. R_f = 0.44 (petroleum ether/ethyl acetate/methanol, 1:1:1/2). Yield: 1.8 g (72%); mp 192–194 °C; ^{1}H NMR (DMSO-d_6) δ 6.45 (s, 1H, CH), δ 7.48–8.05 (m, 13H, Aromatic protons), 8.32 (br, NH_2, D_2O exchangeable), 12.55 (br, NH, benzimidazole, D_2O exchangeable). IR (cm^{-1}): 3374 (NH), 3318, 3249 (NH_2). MS: *m*/*z* 415.0, 1.3% (M^++2 –NH_2); *m*/*z* 313.0, 4.3% (M^++1—benzimidazole part). Anal. Calcd for $C_{23}H_{17}BrN_4$ (429.06): C, 64.35; H, 3.99; Br, 18.61; N, 13.05. Found: C, 64.38; H, 4.01; Br, 18.59; N, 13.10.

5.1.14. 3-(1*H*-Benzo[*d*]imidazol-2-yl)-1-(4-bromophenyl)-5-phenyl-1*H*-pyrrol-2-amine (6d)

Crystallized from chloroform/methanol (2:5) as a brown powder. R_f = 0.37 (petroleum ether/ethyl acetate/methanol, 1:1:1/2). Yield: 72%; mp 200–202 °C; ^{1}H NMR (DMSO-d_6) δ 6.40(s, 1H, CH pyrrol), δ 6.93–6.91 (m, 5H, Aromatic protons), δ 7.11–7.14 (m, 2H, Aromatic protons), δ 7.43(d, J = 8.4 Hz, 2H, Aromatic protons), δ 7.59(d, J = 8.4 Hz, 2H, Aromatic protons), 8.34 (br, NH_2, D_2O exchangeable), 12.65 (br, NH, benzimidazole, D_2O exchangeable). IR (cm^{-1}): 3423, 3299, 3212 (NH) and (NH_2). MS: *m*/*z* 339.0, 0.02% (M^++2—Ph—NH); *m*/*z* 273.0, 6.2% (M^+—*p*-Br-Ph); *m*/*z* 144, 100.0% [M^++2—*p*-Br-Ph—NH_2—benzimidazole unit +2H], *m*/*z* 143, 48.9% [M^++2—*p*-Br-Ph—NH_2—benzimidazole unit +1H]. Anal. Calcd for $C_{23}H_{17}BrN_4$ (429.06): C, 64.35; H, 3.99; Br, 18.61; N, 13.05 Found: C, 64.37; H, 3.90; Br, 18.67 N, 13.10.

5.1.15. 3-(1*H*-Benzo[*d*]imidazol-2-yl)-1-(3-chlorophenyl)-5-phenyl-1*H*-pyrrol-2-amine (6e)

Crystallized from ethyl acetate/methanol (2:5) as a brown powder. R_f = 0.39 (petroleum ether/ethyl acetate/methanol, 1:1:1/2). Yield: 66%; mp 200–202 °C; ^{1}H NMR (DMSO-d_6) δ 6.51 (s, 1H, CH pyrrol), 7.52–7.49 (m, 5H, 2H benzimidazole +4H Aromatic protons), 7.63–7.60 (m, 4H, Aromatic protons), 7.65 (d, J = 7.65, 2H, Aromatic protons), 7.98 (d, J = 7.65, 2H, Aromatic protons), 8.28 (br, NH_2, D_2O exchangeable), 12.25 (br, NH, benzimidazole, D_2O exchangeable). IR (cm^{-1}): 3331 (NH), 3274, 3258 (NH_2). MS: *m*/*z* 382.0, 0.03% (M^+—2H); *m*/*z* 272.0, 3.5% (M^+—*m*-Cl-Ph); *m*/*z* 143, 59.1% [M^++2 –*m*-Cl-Ph—NH_2—benzimidazole unit + 1H]. Anal. Calcd for $C_{23}H_{17}ClN_4$ (384.11): C, 71.78; H, 4.45; Cl, 9.21; N, 14.56. Found: C, 71.72; H, 4.38; Cl, 9.18; N, 14.51.

5.1.16. 3-(1*H*-Benzo[*d*]imidazol-2-yl)-1-(4-chlorophenyl)-5-phenyl-1*H*-pyrrol-2-amine (6f)

Crystallized from ethyl acetate/methanol (2:5) as a brown powder. R_f = 0.36 (petroleum ether/ethyl acetate/methanol, 1:1:1/2). Yield: 73%; mp 133–135 °C; ^{1}H NMR (DMSO-d_6) δ 6.38 (s, 1H, CH), 7.59–7.33 (m, 13H, Aromatic protons), 8.34 (br, NH_2, D_2O exchangeable), 12.49 (br, NH, benzimidazole, D_2O exchangeable). IR (cm^{-1}): 3411, 3329, 3243, (NH) and (NH_2). MS: *m*/*z* 383.0, 1.7% (M^+—1H). Anal. Calcd for $C_{23}H_{17}ClN_4$ (384.11): C, 71.78; H, 4.45; Cl, 9.21; N, 14.56. Found: C, 71.72; H, 4.48; Cl, 9.29; N, 14.61.

5.1.17. 1,3-Di (1*H*-Benzo[*d*]imidazol-2-yl)-5-phenyl-1*H*-pyrrol-2-amine (6g)

Crystallized from ethyl acetate/methanol (2:5) as a green powder. R_f = 0.42 (petroleum ether/ethyl acetate/methanol, 1:1:1/2). Yield: 74%; mp 160–162 °C; ^{1}H NMR (DMSO-d_6): δ 6.36 (s, 1H, CH), 7.17–7.42 (m, 13H, Aromatic protons), 8.12 (br, NH_2, D_2O exchangeable), 12.78 (br, NH, benzimidazole, D_2O exchangeable). IR (cm^{-1}): 3473, 3333, 3298, 3212, 2(NH) and (NH_2). MS: *m*/*z* 391, 6.12% (M^++1). Anal. Calcd for $C_{24}H_{18}N_6$ (390.16): C, 73.83; H, 4.65; N, 21.52. Found: C, 73.79; H, 4.67; N, 21.56.

5.1.18. 1-((1*H*-Benzo[*d*]imidazol-2-yl)methyl)-3-(1*H*-benzo[*d*]imidazol-2-yl)-5-phenyl-1*H*-pyrrol-2-amine (6h)

Crystallized from ethyl acetate/methanol (2:5) as a brown powder. R_f = 0.41(petroleum ether/ethyl acetate/methanol, 1:1:1/2). Yield: 76%; mp 185–187 °C; ^{1}H NMR (DMSO-d_6) δ 5.11 (s, 1H, CH_2), 6.12 (s, 1H, CH_2), 7.68–7.53 (m, 13H, Aromatic protons), 8.10 (br, NH_2, D_2O exchangeable), 12.65 (br, NH, benzimidazole, D_2O exchangeable). ^{13}C NMR (500 MHz, DMSO-d_6): 23.00, 28.44, 33.65, 36. 01, 114.72, 122.63, 128.47, 129.24, 133.73, 136.84, 136.96, 137. 43, 154.89, 174.39, 198.85, 199.02. IR (cm^{-1}): 3224, 3274, 3086, 3136, 2(NH) and (NH_2), 2208 (CN). MS: *m*/*z* 404.9, 22% (M^+); *m*/*z* 286.1, 0.45% (M^+—Benzimidazole moiety); *m*/*z* 295, 6.6% [M^++2-(NH_2+CN)]. Anal. Calcd for $C_{25}H_{20}N_6$ (404.17): C, 74.24; H, 4.98; N, 20.78. Found: C, 74.20; H, 4.99; N, 20.73.

5.1.19. 3-Amino-1*H*-quinoxalin-2-one (8).[41]

A mixture of *o*-phenylenediamine (0.04 mmol) and ethyl oxamate (0.06 mmol) in pyridine (25 mL) was stirred under reflux for 8 h. The reaction mixture was poured into water and the precipitate formed was filtered off, washed and crystallized from ethanol as a buff powder. R_f = 0.36 (petroleum ether/ethyl acetate/methanol, 1: 1: 0.1).Yield: 95%, mp >300 °C. ^{1}H NMR (500 MHz, DMSO-d_6): 7.25(m, 4H); 11.21(br., 2H, NH_2, D_2O exchangeable), 13.19(br, 1H, NH, D_2O exchangeable). ^{13}C NMR (500 MHz, DMSO-d_6): 115.85, 123.95, 125.8, 129.1, 131.6, 142.7, 155.3, 157.5. IR (cm^{-1}): 3492.45(NH quinoxaline), 3288, 3208 (NH_2), 3050, 2968 (CH, aromatic), 1682 (C=O), 1613 (C=N), 1529 (C=C). MS: [*m*/*z* (rel. abundance)]: 161(M^+, 100%). Anal. Calcd for $C_8H_7N_3O$ (FW: 161.16): C, 59.62; H, 4.38; N, 26.07. Found: C, 59.58; H, 4.41; N, 26.19.

5.1.20. 6,12-Dihydro-5,6,11,12-tetraaza-benzo[4,5]cyclohepta[1,2-*b*]naphthalene-13-one (10)

A mixture of anthranilic acid (0.012 mol) and compound **8** (0.012 mol) was heated on a sand path at 120–130 °C for 4 h. Subsequently the melt was allowed to cool for 30 min. at room temperature during this period the melted was solidified. It was treated with an aqueous solution of sodium bicarbonate (10%) in order to dissolve any unreacted acid into the cyclized product. The solid was filtered off and washed with water in order to remove any inorganic materials and recrystallized from ethanol as a green powder. R_f = 0.74 (petroleum ether/ethyl acetate, 2:1). Yield: 84%; mp 168–170 °C; ^{1}H NMR (DMSO-d_6) δ 7.5–7.2 (m, 4H, H2+H3+H9+H10), 7.7–7.6 (m, 4H, H1+H4+H8+H11), 9.41 (s, 1H, NH, D_2O exchangeable). IR (cm^{-1}): 3370 (NH), 3316 (NH), bonded OH centered at 2911, 1675 (C=O), 1592 (C=N). MS: *m*/*z* 263, 24% (M^++1); *m*/*z* 237, 100% (M^++2—CO). Anal. Calcd for $C_{15}H_{10}N_4O$ (262.09): C, 68.69; H, 3.84; N, 21.36. Found: C, 68.76; H, 3.79; N, 21.41.

5.1.21. 6-((1*H*-Benzo[*d*]imidazol-2-yl)methyl)-6,12-dihydro-5,6,11,12-tetraaza-benzo[4,5]cyclohepta[1,2-*b*]naphthalene-13-one (12)

To a stirred solution of compound **10** (4 g, 0.015 mol) and anhydrous potassium carbonate (2.1 g, 0.015 mol) in *N*,*N*-dimethylformamide (30 mL), 2-chloromethylbenzimidazole[42] (2.32 g, 0.015 mol) was added and the reaction mixture was stirred for 8 h at room temperature, then poured onto ice water. The obtained precipitate was filtered off, dried and recrystallized from ethanol as a green powder. R_f = 0.31 (petroleum ether/ethyl acetate, 2:1). Yield: 1.8 g (65%); mp 181–183 °C; ^{1}H NMR (DMSO-d_6) δ: 4.51 (s, 2H, CH2), 7.49–7.01 (m, 10H, Aromatic protons), 8.12 (d, *J* = 8.4 Hz, 2H), 9.36 (s, 1H, NH, D_2O exchangeable), 12.78 (br, NH, benzimidazole, D_2O exchangeable). IR (cm^{-1}): 3368 (NH), 1673 (C=O), 1592 (C=N). MS: *m*/*z* 394, 1.4% (M^++2); *m*/*z* 261, 3.1% (M^+—benzimidazole part—CH_2). Anal. Calcd for $C_{23}H_{16}N_6O$ (392.14): C, 70.40; H, 4.11; N, 21.42. Found: C, 70.35; H, 4.13; N, 21.38.

5.1.22. General procedure for the preparation of compounds (13, 14)

To a solution of compound **12** (0.005 mol) and anhydrous potassium carbonate (0.005 mol) in *N*,*N*-dimethylformamide (30 mL), allyl bromide or ethylbromoacetate (0.005 mol) was slowly added dropwise. The mixture was stirred at room temperature for 5 h, the mixture was then poured onto ice water, and the resulting precipitate was collected by filtration and recrystallized from appropriate solvent.

5.1.23. [2-(13-Oxo-12,13-dihydro-5,6,11,12-tetraaza-benzo[4,5]cyclohepta[1,2-*b*]naphth-6-ylmethyl)-benzimidazol-1-yl]prop-1-ene (13)

Crystallized from ethanol as a brown powder. R_f = 0.61 (petroleum ether/ethyl acetate, 2:1). Yield: 72%; mp 98—100 °C; ^{1}H NMR (DMSO-d_6) δ 5.12 (d, *J* = 4.56, 2H, CH_2), 5.42(m, 2H, =CH_2), 6.05(m, 1H, =CH), 7.05–8.45 (m, 10H, Aromatic Protons), 8.16 (d, *J*=8.11, 2H), 9.54 (s, 1H, NH, D_2O exchangeable). IR (cm^{-1}): 3325 (NH), 1653 (CO). MS: *m*/*z* 277, 100.0% (M^++2—propene group—benzimidazole part); *m*/*z* 263, 1.2% (M^+—propene group—benzimidazole part—CH_2). Anal. Calcd for $C_{26}H_{20}N_6O$ (432.17): C, 72.21; H, 4.66; N, 19.43. Found: C, 72.37; H, 4.58; N, 19.49.

5.1.24. [2-(13-Oxo-12,13-dihydro-5,6,11,12-tetraaza-benzo[4,5]cyclohepta[1,2-*b*]naphth- alene-6-ylmethyl)-benzimidazol-1-yl]-acetic acid ethyl ester (14)

Crystallized from ethanol as a brown powder. R_f = 0.44 (petroleum ether/ethyl acetate, 2:1). Yield: 70%; mp 121—123 °C; ^{1}H NMR (DMSO-d_6) δ 1.02–1.2 (t, 3H, CH_3), 4.16 (s, 2H, $COCH_2$), 4.53 (q, 2H, OCH_2), 5.18 (s, 2H, CH_2), 7.03–8.34 (m, 10H, Aromatic Protons), 8.11 (d, *J* = 8.11, 2H), 9.43 (s, 1H, NH, D_2O exchangeable). IR (cm^{-1}): 3302 (NH), 1741 (OCO), 1682 (CO amide). MS: *m*/*z* 479, 1.6% (M^++1); *m*/*z* 389, 1.3% (M^+—$C_2H_5OCOCH_2$—2H). Anal. Calcd for $C_{27}H_{22}N_6O_3$ (478.18): C, 67.77; H, 4.63; N, 17.56. Found: C, 67.72; H, 4.55; N, 17.52.

5.2. Antitumor activity

5.2.1. Cytotoxicity against lung cancer cell line A549

Cell culture cytotoxicity assays were performed using the alamarBlue method, as previously described.[42] Briefly, aliquots of 100 μL of cell suspension (1.0–2.5 × 10^3 cells) were placed in 96-well microtiter plates in an atmosphere of 5% CO_2 at 37 °C. After 24 h, 100 μL of culture medium and 2 μL of compound in vehicle (culture media with 40% pyridine) or vehicle alone were added, and the plates incubated an additional 72 h. The final pyridine concentration in all cases was 0.4%; at this pyridine concentration, there was no effect on the growth of cells compared to cells in culture media without added pyridine. Compounds, along with mitomycin C as positive control, were evaluated in duplicate at final concentrations ranging from 0.001 to 100 μM. After the culture media had been removed from each well, 200 μL of fresh media

and 20 μL of 90% alamarBlue reagent were added, followed by additional 6 h incubation. The fluorescent intensity was measured using a SpectrafluorPlus plate reader with excitation at 530 nm and emission at 590 nm. Results are reported as IC_{50} values, the average concentration required to produce a decrease of fluorescent intensity of 50% relative to vehicle-treated controls in two separate determinations.

5.2.2. Cytotoxicity against Breast cancer MCF-7 cell line

The antitumor activity against MCF-7 was performed in the National Cancer Institute, Cancer Biology Department, Cairo, Egypt. Potential cytotoxicity of compounds **4g**,**h**, **6a–h**, **10–14** was tested using the method of Skehan et al.[44] Cells were plated in 96-multiwell plate (10^4 cells/well) for 24 h before treatment with the compounds to allow attachment of cell to wall of the plate. Different concentrations of the compound under test (0, 1, 2.5, 5 and 10 μg/mL) were added to the cell monolayer. Triplicate wells were prepared for each individual dose. Monolayer cells were incubated with the compounds for 48 h at 37 °C and in atmosphere of 5% CO_2. After 48 h cells were fixed, washed and stained with Sulforhodamine B stain. Excess stain was washed with acetic acid and attached stain was recovered with Tris EDTA buffer. Color intensity was measured in an ELISA reader. The relation between surviving fraction and drug conc. is plotted to get the survival curve of each tumor cell line after the specified compound.

5.2.3. Antitumor promoting effect in vitro (Epstein–Barr virus activation test)

Compounds **4g**, **4h**, **6a–h**, **8**,**10**,**12**,**13** and **14** were tested for Epstein–Barr virus (EBV) Inhibitory Activity. The inhibition of EBV-EA activation was assayed using methods reported in the literature.[46–48] The cells were incubated at 37 °C for 48 h in a medium containing butyric acid (4 nM), TPA (32 pM), and various amounts of test compounds. Smears were made from the cell suspensions and the EBV-EA inducing cells were stained using an indirect immunofluorescence technique. In each assay, at least 500 cells were counted, and the number of stained cells (positive cells) was recorded. Triplicate assays were per-formed for each data point. The EBV-EA inhibitory activity of the test compound was compared with that of the control experiment with butyric acid plus TPA.

In control experiments, the EBV-EA inhibitory activities were generally around 40%, and these values were taken as a positive control. The viability of the cells was assayed by the Trypan-blue staining method. For the determination of cytotoxicity, the cell viability was required to be more than 60%.

5.3. Molecular docking study

The docking studies were carried out using Molecular Operating Environment (MOE) 2008.10. First, a Gaussian Contact surface around the binding site was drawn. This surface surrounds the van der Waals surface of a molecule (filling in solvent inaccessible gaps). Then docking studies were carried out to evaluate the binding free energy of the inhibitors within the macromolecules. The Dock scoring in MOE software was done using London dG scoring function and has been enhanced by using two different refinement methods, the Forcefield and GridMin pose have been updated to ensure that refined poses satisfy the specified conformations. We allowed rotatable bonds; the best 10 poses were retained and analyzed for the binding poses best score. The database browser was used in MOE to compare the docking poses to the ligand in the co-crystallized structure and to compare the docking pose of the synthesized compounds to the co-crystal ligand position.

5.3.1. Preparation of ligands and target Urokinase plasminogen activator (uPA) receptors

The compounds involved in this study as ligands are compounds which were studied for their binding affinity into Urokinase plasminogen activator (uPA) receptors. The Molecule Builder tool in MOE was used to construct a three-dimensional model of the structures .Energy minimization was done through Force field MMFF94x Optimization using gradient of 0.0001 for determining low energy conformations with the most favorable (lowest energy) geometry.

The crystal structures of uPA receptors were obtained from the Protein Data Bank http://www.rcsb.org/pdb/Welcome.do (PDB code: 1c5x). Hydrogens and partial charges were added to the protein with the Protonate3D application in MOE. This application is to assign ionization states and position hydrogens in the macromolecular structure.

As most of protein structures obtained from the Protein Data Bank contain little or no hydrogen coordinate data due to limited resolution. Yet, the hydrogen bond network and ionization states can have a dramatic effect on simulations results.

5.3.2. Molecular modeling and analysis of the docked results

The binding free energy was used to rank the binding affinity of the synthesize compounds to uPA receptor. Also, Hydrogen bonds between the ligand and amino acids in uPA receptors were used in the ranking of the compounds. Evaluation of the hydrogen bonds was done by measuring the hydrogen bond length which doesn't exceed 3 Å. The mode of interaction of the native ligand uPA receptors within their crystal structures was used as a standard docked model as well as for RMSD calculation.

5.4. Determination the level of uPA protein expression

The level of uPA protein expression was determined using AssayMax human urokinase (uPA) ELISA kit (Assaypro, USA) according to manufacturer's instructions, with absorption measured at 450 nm. Compounds **4h**, **6b** and **13** as well as standards were incubated for 48 h with A549 and MCF7 cells at concentration ranging from 0 to IC_{50} values of each compound which shown in Tables 5 and 6.

After 48 h from compounds treatment, medium was collected and centrifuged at 2000× *g* for 10 min to remove cellular debris. Add 50 μl of the cell extract per well and incubate for 2 h. Wells were washed with 200 μl of wash buffer then add 50 μl of biotinylated uPA antibody to each well and incubate for 1 h at 25 °C. After washing, plates were incubated with 50 μl of streptavidin-peroxidase conjugate per well and incubate for 30 min then wash the microplate as described above. Add 50 μl of chromogen substrate per well and incubate for about 10 min or till the optimal blue color density develops. Add 50 μl of stop solution to each well. The color will change from blue to yellow. Read the absorbance on a microplate reader at a wavelength of 450 nm immediately. The concentrations of uPA in the samples were determined based on the uPA standard curves (0–12 ng).

Acknowledgements

This study was supported by the *'US–Egypt Joint Science and Technology Board Fund*' administered through the USDA (BIO9-002-015). The authors are grateful to the National Cancer Institute, Cancer Biology Department, Cairo, Egypt, to perform the antitumor activity against MCF-7. Deep thanks are expressed to the 'Science & Technology Development Fund' for financially supporting the manuscript through the fund of the STDF project No 1517.

References and notes

1. Abdel-Mohsen, H. T.; Ragab, F. A. F.; Ramla, M. M.; El Diwani, H. I. *Eur. J. Med. Chem.* **2010**, *4*, 2336.
2. Galal, S. A.; Kassab, A. S.; Rodriguez, M. L.; Kerwin, S. M.; El Diwani, H. I. *Eur. J. Chem.* **2010**, *2*, 67.
3. Galal, S. A.; Hegab, K. H.; Kassab, A. S.; Rodriguez, M. L.; Kerwin, S. M. *Eur. J. Med. Chem.* **2009**, *44*, 1500.
4. Ramla, M. M.; Omar, M. A.; El-Khamry, Abdel-M. M.; El Diwani, H. I. *Bioorg. Med. Chem.* **2006**, *14*, 7324.
5. El-Naem, Sh. I.; El-Nazhawy, A. O.; El-Diwani, H. H.; Abdel Hamid, A. O. *Arch. Pharm. Pharm. Med. Chem.* **2003**, *1*, 7.
6. El-Naem, Sh. I.; El-Nazhawy, A. O.; El-Diwani, H. H.; Abdel Hamid, A. O. *Mans. Sci. Bull. (A chem.)* **2002**, *28*, 325.
7. Ramla, M. M.; Omar, M. A.; Tokuda, H.; El-Diwani, H. I. *Bioorg. Med. Chem.* **2007**, *15*, 6489.
8. Gravatt, G. L.; Baguley, B. C.; Wilson, W. R.; Denny, W. A. *J. Med. Chem.* **1994**, *37*, 4338.
9. Alper, S.; Arpaci, Ö. T.; Aki, E. Ş.; Yalcin, I. *Farmaco* **2003**, *58*, 497.
10. Sun, Q.; Gatto, B.; Yu, C.; Liu, A.; Liu, L. F.; LaVoie, E. J. *J. Med. Chem.* **1995**, *38*, 3638.
11. Sun, Q.; Gatto, B.; Yu, C.; Liu, A.; Liu, L. F.; LaVoie, E. J. *Bioorg. Med. Chem. Lett.* **1994**, *4*, 2871.
12. Corbett, A. H.; Guerry, P.; Pflieger, P.; Osheroff, N. *Antimicrob. Agents Chemother.* **1993**, *37*, 2599.
13. McClure, K. J.; Huang, L.; Arienti, K. L.; Axe, F. U.; Brunmark, A.; Blevitt, J.; Breitenbucher, J. G. *Bioorg. Med. Chem. Lett.* **1924**, *2006*, 16.
14. Neff, D. K.; Lee-Dutra, A.; Blevitt, J. M.; Axe, F. U.; Hack, M. D.; Buma, J. C.; Rynberg, R.; Brunmark, A.; Karlsson, L.; Breitenbucher, G. *Bioorg. Med. Chem. Lett.* **2007**, *17*, 6467.
15. Arienti, K. L.; Brunmark, A.; Axe, F. U.; McClure, K.; Lee, A.; Blevitt, J.; Neff, D. K.; Huang, L.; Crawford, S.; Pandit, C. R.; Karlsson, L.; Breitenbucher, J. G. *J. Med. Chem.* **1873**, *2005*, 48.
16. Hornberger, K. R.; Badiang, J. G.; Salovich, J. M.; Kuntz, K. W.; Emmitte, K. A.; Cheung, M. *Tetrahedron Lett.* **2008**, *49*, 6348.
17. Duffy, M. J. *Curr. Pharm. Des.* **2004**, *10*, 39.
18. Syrovets, T.; Simmet, T. *Cell. Mol. Life Sci.* **2004**, *61*, 873.
19. Duffy, M. J. *Fibrinolysis* **1993**, *7*, 295.
20. Mignatti, P.; Rifkin, D. B. *Physiol. Rev.* **1993**, *73*, 161.
21. Bdeir, K.; Kuo, A.; Sachais, B. S.; Rux, A. H.; Bdeir, Y.; Mazar, A.; Higazi, A. A.; Cines, D. B. *Blood* **2003**, *102*, 3600.
22. Blasi, F.; Carmeliet, P. *Nat. Rev. Mol. Cell Biol.* **2002**, *3*, 932.
23. Andreasen, P. A.; Kjoller, L.; Christensen, L.; Duffy, M. J. *Int. J. Cancer* **1997**, *72*, 1.
24. Meyer, T.; Hart, I. R. *Eur. J. Cancer* **1998**, *34*, 214.
25. Sidenius, N.; Blasi, F. *Cancer Metastasis Rev.* **2003**, *22*, 205.
26. Duffy, M. J.; Duggan, C. *Clin. Biochem.* **2004**, *37*, 541.
27. Penning, T. D.; Zhu, G.; Gandhi, V. B.; Gong, J.; Thomas, Sh.; Lubisch, W.; Grandel, R.; Wernet, W.; Park, C. H.; Fry, E. H.; Liu, X.; Shi, Y.; Klinghofer, V.; Johnson, E. F.; Donwho, C. K.; Forst, D. J.; Bontcheva-Diaz, V.; Bouska, J. J.; Olson, A. M.; Marsh, K. C.; Luo, Y.; Rosenberg, S. H.; Giranda, V. L. *Bioorg. Med. Chem.* **2008**, *16*, 6965.
28. Starčević, K.; Kralj, M.; Ester, K.; Sabol, I.; Grce, M.; Pavelić, K.; Karminski-Zamola, G. *Bioorg. Med. Chem.* **2007**, *15*, 4419.
29. Mackman, R. L.; Hui, H. C.; Breitenbucher, J. G.; Katz, B. A.; Luong, C.; Martelli, A.; McGee, D.; Radika, K.; Sendzik, M.; Spencer, J. R.; Sprengeler, P. A.; Tario, J.; Verner, E.; Wang, J. *Bioorg. Med. Chem. Lett.* **2002**, *12*, 2019.
30. Hajduk, P. J.; Boyd, S.; Nettesheim, D.; Nienaber, V.; Severin, J.; Smith, R.; Davidson, D.; Rockway, T.; Fesik, S. W. *J. Med. Chem.* **2000**, *43*, 3862.
31. Alonso, D. F.; Tejera, A. M.; Farias, E. F.; Joffe, E. B. D.; Gomez, D. E. *Anticancer Res.* **1998**, *18*, 4499.
32. Rabbani, S. A.; Harakidas, P.; Davidson, D. J.; Henkin, J.; Mazar, A. P. *Int. J. Cancer* **1995**, *63*, 840.
33. Xing, R. H.; Mazar, A. P.; Henkin, J.; Rabbani, S. A. *Cancer Res.* **1997**, *57*, 3585.
34. Evans, D. M.; Sloan-Stakleff, K. D. *Invasion Metastasis* **1998/99**, *18*, 252.
35. Spencer, J. R.; McGee, D.; Allen, D.; Katz, B. A.; Luong, C.; Sendzik, M.; Squires, N.; Mackman, R. L. *Bioorg. Med. Chem. Lett.* **2002**, *12*, 2023.
36. Bridges, A. J.; Lee, A.; Schwartz, C. E.; Towle, M. J.; Littlefield, B. A. *Bioorg. Med. Chem.* **1993**, *1*, 403.
37. Abdelhamid, A. O.; Negm, A. M.; Abass, I. M. *J. Parkt. Chem.* **1989**, *33*, 31.
38. Hilmy, K. M.; Pedersen, E. B. *Liebigs Ann. Chem.* **1989**, 1145.
39. Galal, S. A.; Abdelsamie, A. S.; Tokuda, H.; Suzuki, N.; Lida, A.; ElHefnawi, M. M.; Ramadan, R. A.; Atta, M. H. E.; El Diwani, H. I. *Eur. J. Med. Chem.* **2011**, *46*, 327.
40. Tiwari, A. K.; Mishra, A. K.; Singh, V. K. *Bioorg. Med. Chem. Lett.* **2006**, *16*, 4581.
41. Skolnik, B. H.; Miller, J. G.; Day, A. R. *J. Am. Chem. Soc.* **1854**, *1943*, 65.
42. Ahmed, S. A.; Gogal, R. M.; Walsh, J. E. *J. Immunol. Methods* **1994**, *170*, 211.
43. Skehan, P.; Storeng, R.; Scudiero, D.; Monks, A. *J. Natl. Cancer Inst.* **1990**, *82*, 1107.
44. Iranshahi, M.; Sahebkar, A.; Hosseini, S. T.; Takasaki, M.; Konoshima, T.; Tokuda, H. *Phytomedicine* **2010**, *17*, 269.
45. Ito, Y.; Kawanishi, M.; Harayama, T.; Takabayashi, S. *Cancer Lett.* **1981**, *12*, 175.
46. Takasaki, M.; Konoshima, T.; Kuroki, S.; Tokuda, H.; Nishino, H. *Cancer Lett.* **2001**, *173*, 133.
47. Konoshima, T.; Takasaki, M.; Kozuka, M.; Tokuda, H. *J. Nat. Prod.* **1987**, *50*, 1167.
48. Molecular Operating Environment (MOE) 2008.10, Chemical Computing Group Inc., Quebec, Canada, 2008.